

Optical and Electrical Studies of Graphene Deposited on GaN Nanowires

J. KIERDASZUK^a, P. KAŻMIERCZAK^a, A. DRABIŃSKA^a, A. WYSMOŁEK^a, K. KORONA^a,
M. KAMIŃSKA^a, K. PAKUŁA^a, I. PASTERNAK^b, A. KRAJEWSKA^{b,c} AND Z.R. ŻYTKIEWICZ^d

^aFaculty of Physics, University of Warsaw, Warszawa, Poland

^bInstitute of Electronic Materials Technology, Warszawa, Poland

^cInstitute of Optoelectronics, Military University of Technology, Warszawa, Poland

^dInstitute of Physics, Polish Academy of Sciences, Warszawa, Poland

In this paper using scanning electron microscope, contactless microwave electronic transport and the Raman spectroscopy we studied the properties of graphene deposited on GaN nanowires and compared it with the graphene deposited on GaN epilayer. The Raman micro-mapping showed that nanowires locally change the strain and the concentration of carriers in graphene. Additionally we observed that nanowires increase the intensity of the Raman spectra by more than one order of magnitude.

DOI: [10.12693/APhysPolA.126.1087](https://doi.org/10.12693/APhysPolA.126.1087)

PACS: 81.05.ue, 72.10.Fk, 78.67.Wj, 72.80.Vp

1. Introduction

Solar light is converted into electricity in environmental friendly photovoltaic devices — solar cells. Recently much effort has been put in development of organic solar cells. One of the basic requirements of solar cells is transparent front electrode for which indium tin oxide (ITO) is one of the most widely used material nowadays [1]. ITO transmission reaches 80% and its conductivity is about $10^{-4} \Omega\text{cm}$ [2]. Because of high price of indium it is considered to replace ITO by other materials, among which graphene is one of the most serious options. The advantage of using graphene as an electrode material in solar cell is its high transparency (up to almost 99%) [3], remarkably strong for its very low weight, high thermal and electrical conductance and systematic price decrease [4–6]. On the other hand, it has been shown recently that efficiency of organic solar cells can be substantially increased by using nanowire structures [7]. Therefore nanowires (NWs) covered from the top with graphene seems to be an interesting system for solar cells architecture.

2. Sample preparation

We studied two samples: graphene deposited on GaN NWs (NWs graphene) and reference sample of graphene deposited on GaN epilayer (EPI graphene). GaN NWs were grown on Si(111) substrate by plasma assisted molecular beam epitaxy technique without use of any catalyst in N-rich growth conditions [8]. Scanning electron microscope (SEM) showed that NWs were about one μm high, width of hundred nm and almost vertical with a small tilt. Sometimes, however, nearest neighbours were connected in the upper parts.

Graphene was grown using chemical vapour deposition (CVD) technique on copper substrate with propane gas as a precursor. The process of transferring graphene onto

GaN epilayer was done by means of substrate standard method using poly(methyl methacrylate) (PMMA) [9], whereas for GaN NWs we applied polymer-free transferring method [10].

3. Contactless microwave electrical transport measurements

Contactless microwave electrical transport measurements were carried out using a Bruker ELEXSYS E580 spectrometer [11]. For both samples magnetoconductance feature at low magnetic field is observed. For EPI graphene line is higher and sharper than for NWs graphene (Fig. 1a). The observed signal can be understood by considering suppression of conductivity caused by positive quantum interference of carriers in graphene. This leads to the enhancement of backscattering probability called weak localization. In this case measured derivative conductivity dependence on magnetic field is represented by equation [12]:

$$\frac{d\sigma(B)}{dB} = \frac{e^2}{\pi h} \left[\frac{1}{B_\varphi} F' \left(\frac{B}{B_\varphi} \right) - \frac{1}{B_\varphi + 2B_i} F' \left(\frac{B}{B_\varphi + 2B_i} \right) - \frac{2}{B_\varphi + B_i + B_{lr}} F' \left(\frac{B}{B_\varphi + B_i + B_{lr}} \right) \right], \quad (1)$$

where $F'(B) = \frac{1}{B} + \frac{1}{B^2} \psi' \left(\frac{1}{2} + \frac{1}{B} \right)$ and ψ' is trigamma function. Using equation: $L_{\varphi, i, lr} = \sqrt{\frac{\hbar}{8\pi e B_{\varphi, i, lr}}}$ we calculated coherence length (L_φ), elastic intervalley scattering length (L_i), and elastic intravalley (long range) scattering length (L_{lr}) for both samples (Table). It was found that both coherence and elastic intervalley lengths are strongly reduced for NWs graphene comparing to the EPI graphene. The temperature dependence of the coherence length can give information about the nature of inelastic scattering responsible for decoherence. Both samples were characterized as a function of temperature. Observation of the characteristic line related to weak-

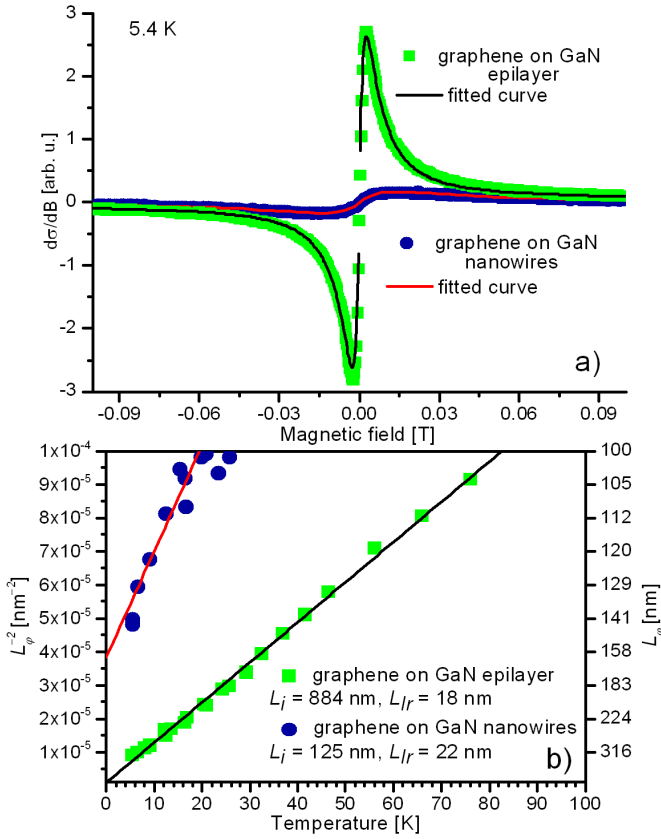


Fig. 1. Results of contactless transport measurements: (a) Comparison of spectrum of graphene deposited on GaN NWs and on GaN epilayer, (b) Linear dependence of $L_\phi^{-2}(T)$ in sample of graphene deposited on GaN NWs and GaN surface.

localization in graphene showed the reduction of the coherence length from about 150 nm at 5 K to 100 nm at 20 K for NWs graphene and from 330 nm at 5 K to 104 nm at 80 K for EPI graphene (Fig. 1b). Intervalley and intravalley elastic scattering were found to be independent on temperature. In each sample we observed linear dependence of $L_\phi^{-2}(T)$ which can be understood as a case of electron–electron scattering in diffusive regime. After fitting linear functions we observed that in NWs graphene nonzero offset is clearly present. It indicates the presence of additional inelastic scattering process in NWs graphene, which is independent of temperature and reduces coherence length from infinite to finite value at absolute zero temperature.

4. Raman results

The Raman spectroscopy of NWs graphene was carried out using T64000 Horiba Jobin-Yvon spectrometer with Nd:YAG laser operating at 532 nm wavelength as an excitation source. It was found that proximity of GaN NWs substantially increases intensity of graphene Raman spectra, by more than one order of magnitude as compared to as grown CVD material, as well as to EPI graphene

TABLE

Scattering lengths [nm] obtained from WL fit, grain diameters, and distance between defects obtained from Raman measurement in graphene deposited on GaN NWs and GaN surface.

Graphene deposited on	NWs #1	epilayer #2	ratio #2/#1
coherence scattering length (L_ϕ) at 2 K	142	330	2.3
coherence scattering length (L_ϕ) extrapolated to 300 K	32	53	1.7
intervalley scattering length (L_i)	125	884	7.1
intravalley scattering length (L_{lr})	22	18	0.8
grain diameter (L_α)	9	27	3.0
distance between defects (L_D)	8	14	1.8

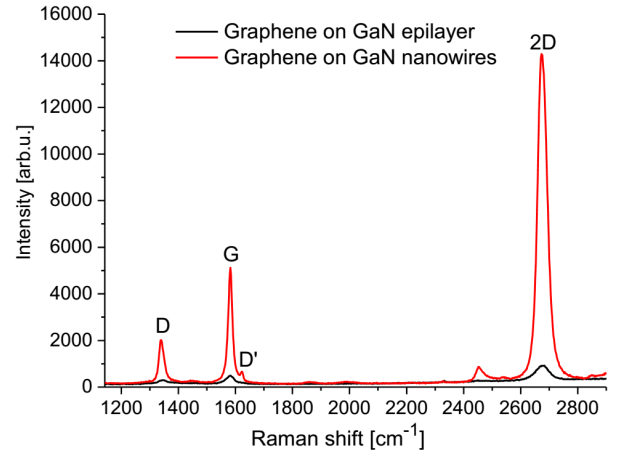


Fig. 2. Comparison of Raman spectrum of graphene deposited on nanowires and on GaN epilayer.

(Fig. 2). As can be seen from the Raman mapping experiment, the observed changes of spectrum (peak positions, widths and intensities) unambiguously correlate with the positions of individual NWs (Fig. 3a and b). This shows that NWs introduced strain to graphene layer and changed the concentration of carriers in it.

The observed intensity ratio of G peak to D peak for NWs graphene seems to be not correlated with GaN NWs pattern (Fig. 3c) and average value (0.46) was smaller comparing to the EPI graphene for which the average ratio was 1.38. This suggests large enhancement of the defect related scattering processes rather than defect generation by NWs.

Using intensity ratio of G peak to D peak (I_G/I_D) it is possible to calculate the average grain diameter and distance between defects [13, 14]. The average grain diameter can be estimated by

$$L_\alpha [\text{nm}] = 2.4 \times 10^{-10} [\text{nm}^{-3}] \lambda^4 \frac{I_G}{I_D}. \quad (2)$$

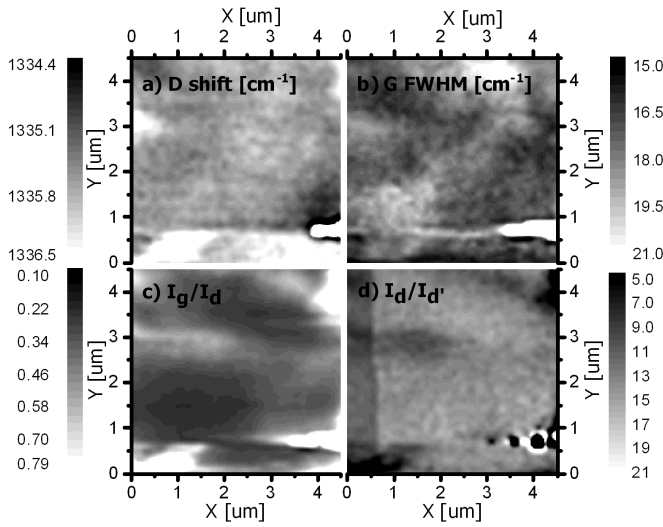


Fig. 3. Raman spectroscopy results: (a) D peak energy, (b) G peak FWHM, (c) ratio of G peak and D peak intensities, (d) ratio of D and D' peak intensities.

The average distance between defects can be estimated by

$$L_D^2 [\text{nm}^2] = 1.8 \times 10^{-9} [\text{nm}^{-2}] \lambda^4 \frac{I_G}{I_D}, \quad (3)$$

where λ is wavelength of laser in nm. From the Raman measurements we calculated average I_G/I_D ratio for NWs graphene and EPI graphene and furthermore the average grain diameter or distance between defects. We compared these values with elastic scattering lengths and decoherence length extrapolated to 300 K obtained from transport measurements (Table). In both samples coherence lengths are similar to distance between defects calculated from the Raman results.

5. Summary

In this work we studied defect scattering in graphene deposited on GaN NWs by means of contactless microwave-induced electron transport and the Raman spectroscopy. Analysing weak localization, we observed reduction of scattering lengths in NWs graphene comparing to EPI graphene. Temperature independent inelastic scattering responsible for decoherence, reducing the decoherence length at 0 K, was found in NWs graphene. Increase of intensity of graphene Raman spectra by one order of magnitude in the sample of NWs graphene was observed. Nanowires changed the intensity of Raman spectra of graphene locally, but the observed defects in NWs graphene seemed to be homogeneously distributed.

Acknowledgments

This work was partially supported by the NCN grant no 2012/07/B/ST3/03220, Poland and NCBiR grant GRAF TECH/NCBR/02/19/2012, Poland. Z.R.Z. is grateful for support from the grant Innovative Economy POI G.01.03.01 00-159/08 (InTechFun).

References

- [1] H. Schmidt, H. Flügge, T. Winkler, T. Bülow, T. Riedl, W. Kowalsky, *Appl. Phys. Lett.* **94**, 243302 (2009).
- [2] H. Kim, C.M. Gilmore, A. Piqué, J.S. Horwitz, H. Mattoussi, H. Murata, Z.H. Kafafi, D.B. Chrisey, *J. Appl. Phys.* **86**, 6451 (1999).
- [3] R.R. Nair, P. Blake, A.N. Grigorenko, K.S. Novoselov, T.J. Booth, T. Stauber, N.M.R. Peres, A.K. Geim, *Science* **320**, 1308 (2008).
- [4] C. Lee, X. Wei, J.W. Kysar, J. Hone, *Science* **321**, 385 (2008).
- [5] A.A. Balandin, S. Ghosh, W. Bao, I. Calizo, D. Teweldebrhan, F. Miao, C.N. Lau, *Nano Lett.* **8**, 902 (2008).
- [6] S.V. Morozov, K.S. Novoselov, M.I. Katsnelson, F. Schedin, D.C. Elias, J.A. Jaszczak, A.K. Geim, *Phys. Rev. Lett.* **100**, 016602 (2008).
- [7] P. Krogstrup, H.I. Jorgensen, M. Heiss, O. Demichel, J.V. Holm, M. Aagesen, J. Nygard, A. Fontcuberta i Morral, *Nature Photon* **7**, 306 (2013).
- [8] A. Wierzbička, Z.R. Zytkiewicz, S. Kret, J. Borysiuk, P. Dłuzewski, M. Sobanska, K. Kłosek, A. Reszka, G. Tchutchulashvili, A. Cabaj, E. Lusakowska, *Nanotechnology* **24**, 035703 (2013).
- [9] T. Ciuk, I. Pasternak, A. Krajewska, J. Sobieski, P. Caban, J. Szmidt, W. Strupinski, *J. Phys. Chem. C* **117**, 20833 (2013).
- [10] I. Pasternak, A. Krajewska, K. Grodecki, I. Jozwik-Biała, K. Sobczak, W. Strupinski, *AIP Adv.* **4**, 097133 (2014).
- [11] A. Drabinska, A. Wolos, M. Kaminska, W. Strupinski, J.M. Baranowski, *Phys. Rev. B* **86**, 045421 (2012).
- [12] E. McCann, K. Kechedzhi, V.I. Fal'ko, H. Suzuura, T. Ando, B.L. Altshuler, *Phys. Rev. Lett.* **97**, 146805 (2006).
- [13] A. Eckmann, A. Felten, A. Mishchenko, L. Britnell, R. Krupke, K.S. Novoselov, C. Casiraghi, *Nano Lett.* **12**, 3925 (2012).
- [14] F. Tuinstra, L. Koenig, *J. Chem. Phys.* **53**, 1126 (1970).
- [15] L.G. Cançado, A. Jorio, E.H. Martins Ferreira, F. Stavale, C.A. Achete, R.B. Capaz, M.V.O. Moutinho, A. Lombardo, T. Kulmala, A.C. Ferrari, *Nano Lett.* **11**, 3190 (2011).